Available online at website: https://journal.bcrec.id/index.php/bcrec

Bulletin of Chemical Reaction Engineering & Catalysis, 19 (1) 2024, 108-117

Research Article

Optimization of Cu_2O Thickness to Enhance Photocatalytic Properties of Electrodeposited Cu_2O/FTO Photoanode

Riza Ariyani Nur Khasanah[1,2,3,*], Forest Shih-Sen Chien[2], Rita Prasetyowati[1], Rike Yudianti[3]

[1]Department of Physics Education, Universitas Negeri Yogyakarta, Yogyakarta 55281, Indonesia.
[2]Department of Applied Physics, Tunghai University, Taichung 407224, Taiwan.
[3]Research Center for Advanced Materials, National Research, and Innovation Agency (BRIN), Tangerang Selatan 15314, Indonesia.

Received: 7th December 2023; Revised: 6th February 2024; Accepted: 7th February 2024
Available online: 10th February 2024; Published regularly: April 2024

Abstract

Currently, n-type cuprous oxide (Cu_2O) is a promising material as photocatalyst because of its energy gap of 2 eV that absorbs visible light up to a wavelength of 600 nm. As a photoelectrode, the thickness of Cu_2O is crucial, where the improper thickness may worsen the photocatalytic properties. This work aimed to enhance the photocatalytic properties of Cu_2O electrodeposited on fluorine-doped tin oxide (FTO), called Cu_2O/FTO, by optimizing the Cu_2O thickness. The thickness of Cu_2O was controlled by adjusting the deposition time in the electrochemical deposition of Cu_2O/FTO. By changing the deposition time from 5 to 45 min, the morphology of Cu_2O changed from a leaf-like shape to an irregular facet shape with highly dense coverage, and the average thickness increased from 370 to 1100 nm. The increasing Cu_2O thickness resulted in the increasing light absorption. The Cu_2O/FTO demonstrated anodic photocurrent, which increased with the Cu_2O thickness up to a threshold value of 1000 nm (35 min deposition time). At a thickness of 1000 nm, Cu_2O/FTO achieved the highest photocurrent (150 and 58 μA under irradiation of 365 and 470 nm, respectively) due to the highly dense morphology and high absorption. In addition, with a thickness of 1000 nm, the charge diffusion was still good. Further, the increase of Cu_2O film thickness higher than 1000 nm caused low photocatalytic properties even though the morphology was highly dense, and the absorption was the highest. This condition could be due to the relatively too-high resistance of Cu_2O that caused poor charge diffusion.

Keywords: Cu_2O; thickness; photocatalytic properties; electrochemical deposition; deposition time

How to Cite: R.A.N. Khasanah, F.S.S. Chien, R. Prasetyowati, R. Yudianti (2024). Optimization of Cu_2O Thickness to Enhance Photocatalytic Properties of Electrodeposited Cu_2O/FTO Photoanode. *Bulletin of Chemical Reaction Engineering & Catalysis*, 19 (1), 108-117 (doi: 10.9767/bcrec.20081)

Permalink/DOI: https://doi.org/10.9767/bcrec.20081

1. Introduction

Photocatalysis is a field of research that is much in demand because of its application utilizing sunlight energy to produce hydrogen gas (H_2) through photocatalytic water splitting [1] and to overcome water pollution through photocatalytic degradation of pollutants [2]. Cuprous oxide (Cu_2O) is a promising material for photocatalysis that works under visible light irradiation because it has a narrow energy gap (2.0 − 2.6 eV) [3,4]. The valence band (VB) and conduction band (CB) edge positions of Cu_2O coincide with the redox potentials of water. At pH 7, the VB of Cu_2O (0.65 vs. Ag/AgCl) is at a more positive potential than the oxidation potential of H_2O to O_2 (0.62 vs. Ag/AgCl), and the CB of Cu_2O (−1.35 V vs. Ag/AgCl) is at a more negative potential than the reduction potential of H^+ to H_2 (−0.62 vs. Ag/AgCl) [5]. Furthermore, Cu_2O photocatalysis is extremely widespread because it is non-toxic, abundant in nature, and inexpensive [6]. Typically, Cu_2O is a p-type semiconductor because of copper vacancies in the crystal lattice [7,8]. The p-type Cu_2O acts as a photocathode used for photocatalytic reduction reactions [8,9]. Currently, many researchers prepared Cu_2O as an

* Corresponding Author.
Email: rizaariyani@uny.ac.id (R.A.N. Khasanah);
Telp: +62-85-727912651

n-type semiconductor, which is formed due to oxygen vacancies [10–12]. The n-type Cu_2O acts as photoanode and is applied for photocatalytic oxidation reactions [11,12]. The n-type Cu_2O is interesting to study widely because of its application for photocatalytic degradation of dyes that pollute the environment.

Cu_2O can be fabricated using various methods, such as sputtering [13], thermal oxidation [14], chemical immersion [15], electrochemical deposition [16], and others. Among various thin film deposition methods, the electrochemical deposition method is the most popular method for fabricating Cu_2O because it is cheap, highly scalable, and easy to operate. This method can control conductivity type, morphology, facets, and thickness by adjusting electrochemical deposition parameters, such as voltage, time, and solution pH [7]. For example, the fabrication of Cu_2O photoelectrode prepared at pH 6.2 exhibited n-type conductivity, while those obtained at pH 11 showed p-type conductivity [17]. Furthermore, the variation of deposition time can change the morphology and thickness of n-type Cu_2O [18]. Several works have attempted to enhance the photocatalytic performance of n-type Cu_2O by changing the deposition parameters in the electrochemical deposition method [10–12,19]. As a photoelectrode, thickness of Cu_2O film can affect the photon absorption and charge diffusion, where the increase of film thickness can increase the light absorption, but reduce the charge diffusion [20]. Hence, the optimization of the Cu_2O film thickness is crucial to achieve the highest photocatalytic activity of n-type Cu_2O. However, the optimized film thickness of n-type Cu_2O for enhancing its photocatalytic properties has not been studied.

This work aimed to study the threshold thickness of n-type Cu_2O in enhancing the photocatalytic properties of n-type Cu_2O deposited on fluorine-doped tin oxide (FTO) by the electrochemical deposition method. The thickness of Cu_2O was adjusted by controlling the deposition time. The variation of deposition times from 5 to 45 min resulted in the transformation of Cu_2O morphology from a leaf-like shape (thickness of 370 nm) to an irregular faceted shape (thickness of 1100 nm) with a highly dense coverage. The increase of Cu_2O thickness resulted in the increase of light absorption. The Cu_2O with a deposition time of 35 min (thickness of 1000 nm) showed the highest anodic photocurrent response (150 and 58 μA under irradiation with wavelengths of 365 and 470 nm, respectively) among all the investigated Cu_2O, indicating that the threshold film thickness was 1000 nm. In this condition, the Cu_2O, with a thickness of 1000 nm, exhibited a highly dense morphology and high absorption. Additionally, the charge diffusion was still good. The Cu_2O film with a thickness higher than 1000 nm resulted in poor photocatalytic properties even though the morphology was highly dense, and the absorption was the highest. The relatively too-high resistance of Cu_2O with a thickness higher than 1000 nm might cause poor charge diffusion, leading to the poor photocatalytic properties.

2. Materials and Methods

2.1 Preparation of Cu_2O/FTO

Cu_2O film was fabricated using the electrochemical deposition method in a three-electrode cell using an electrochemical workstation (Zahner Zennium, Germany) [12]. The working electrode was FTO, the reference electrode was Ag/AgCl, and the counter electrode was a Pt plate. The electrolyte for the electrodeposition of Cu_2O/FTO was a mixed solution of 0.02 M $Cu(CH_3COO)_2.H_2O$ (Powder, 99.9%, Sigma-Aldrich) and 0.1 M $NaCH_3COO$ (Powder, 99%, Sigma-Aldrich) in 40 mL of deionized (DI) water. The pH of the electrolyte was adjusted to 6.5 via 0.5 M CH_3COOH (Powder, 99.8%, Sigma-Aldrich). Repurification was not required because all chemicals were in good purity. Before deposition began, the FTO was washed using a solution of acetone, ethanol, and DI water in an ultrasonic cleaner sequentially for 10 min each. Next, the electrochemical deposition was carried out at a voltage of −0.2 V vs. Ag/AgCl under different deposition times (5, 15, 25, 35, and 45 min). During the deposition process, the electrolyte temperature was kept constant at 60 °C. After that, the as-prepared sample, called Cu_2O/FTO, was washed using DI water and then dried using nitrogen gas for approximately 5 min.

Cu_2O/FTO was also prepared with a "step height" on its surface for thickness measurement. The sample preparation process followed the same procedure as original Cu_2O/FTO. However, the FTO was modified before the electrodeposition process. A tape (0.5 cm × 1 cm) was attached to the middle of the FTO surface. Next, the electrochemical deposition was carried out at a voltage of −0.2 V vs. Ag/AgCl and electrolyte temperature of 60 °C under different deposition times (5, 15, 25, 35, and 45 min). Once finished, the tape on the FTO surface was peeled off. After that, the as-prepared Cu_2O/FTO having a "step height" was washed using DI water and then dried using nitrogen gas for approximately 5 min.

2.2 Characterization of Cu_2O/FTO

Cu_2O/FTO was characterized using several techniques. Before the characterization, the Cu_2O/FTO was purged with nitrogen gas for approximately 5 min to remove the dust from the surface. The topography of Cu_2O was observed using Atomic Force Microscopy (AFM) (PicoScan-AFM, Molecular Imaging Inc; now known as Agilent Technologies, USA). The thickness of Cu_2O was measured by AFM. For this measurement, the Cu_2O/FTO was prepared in as a step height sample. The crystal structure was recorded using X-ray diffractometry (XRD) (PANalytical X'Pert PRO, Netherlands) at an incidence wavelength of 1.5401 Å (Cu-Kα radiation). The vibration modes were measured using Raman spectroscopy (NTEGRA Spectra, NT-MDT, Netherlands) under excitation of 532 nm-wavelength (2.1 $mW.\mu m^{-2}$). The light absorption spectra were measured using ultraviolet–visible (UV–vis) spectroscopy equipped with an integration sphere and a Xe lamp.

2.3 Measurement of Photocatalytic Properties of Cu_2O/FTO

The photocatalytic properties of Cu_2O/FTO were investigated by measuring the photocurrent under light irradiation with wavelengths of 365 and 470 nm at a light intensity of 5 $mW.cm^{-2}$. The photocurrent measurement was performed using a source meter (Keithley 2400) under a two-electrode cell configuration without a bias. The Cu_2O/FTO acted as the working electrode and a Pt plate acted as the counter electrode. The electrolyte solution was 0.05 M Na_2SO_4. Furthermore, the photocatalytic activity of the Cu_2O/FTO was examined by measuring the degradation of methylene blue (MB) under dark and light irradiation of 365 nm (38 $mW.cm^{-2}$) through monitoring the decrease in absorbance peak of MB solution at a wavelength of 664 nm [21]. The photocatalytic degradation of MB was measured without bias, with an initial MB concentration of 5 μM in the electrolyte of 0.05 M Na_2SO_4.

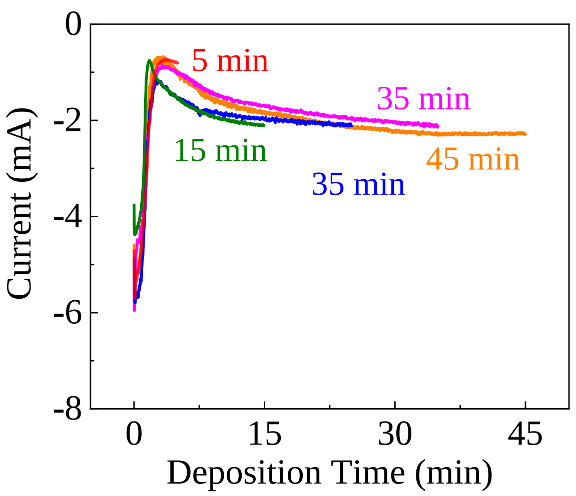

Figure 1. Current of Cu_2O/FTO recorded during electrochemical deposition process under different deposition times.

3. Results and Discussion

3.1 Effect of Deposition Time on Morphology, Thickness, and Properties of Cu_2O/FTO

Cu_2O/FTO was fabricated using an electrochemical deposition method by applying a constant voltage (−0.2 V vs. Ag/AgCl) with varying deposition times from 5 to 45 min. The formation of Cu_2O on the FTO substrate in the solution containing $Cu(CH_3COO)_2$ occurred following the reaction of $2Cu^{2+} + 2OH^- + 2e^- \rightarrow Cu_2O + H_2O$ [22]. During the deposition process, the current resulting from the deposition process was recorded against the deposition time, as seen in Figure 1. The deposition current clearly showed the Cu_2O nucleation-growth step, where there are three regions [23,24]. Initially, the first current region showed that the Cu_2O growth process began with the nucleation of Cu_2O grains on the FTO surface, characterized by a high cathodic current quickly around 30 s because of the conductive FTO with a sheet resistance of 22 Ω/sq [12]. The cathodic current increased rapidly, indicating that the deposition rate of Cu_2O was controlled by surface diffusion of Cu^{2+} with uniform incoming flux [25,26]. After that, as time increased (the second current region), the number of Cu_2O grains increased and covered the FTO surface, causing the higher resistance on the FTO surface, indicated by the decrease of the cathodic current until reaching its maximum before decaying. In this condition, each Cu_2O grains developed in the diffusion zone. In the third current region (more than 5 min), the cathodic current decayed to equilibrium, and the development of Cu_2O material on the FTO surface was more abundant. Finally, Cu_2O material covered the whole surface of FTO. The surface diffusion could control the morphology and roughness of Cu_2O on the FTO surface [26]. The number of Cu_2O material on the FTO surface depended on the deposition times, where the total charge (electric current times deposition time) during the electrochemical deposition process determined the grain number. Hence, the number of Cu_2O grains increased as the deposition time increased, leading to the increase of the Cu_2O film thickness [18].

The topography of Cu_2O/FTO was observed with AFM, presented in Figure 2. The morphology of Cu_2O on the FTO substrate depended on the deposition time. The change in the morphology of Cu_2O corresponded to the form of the deposition current (Figure 1). As shown in Figure 2(a), Cu_2O deposited for 5 min demonstrated three leaf-like grains with dendritic branches of 500 − 800 nm length. The Cu_2O grains deposited on the FTO surface showed branching dendritic development because the surface diffusion of Cu^{2+} in the plating solution could not refill the deposition [24]. This leaf-like shape of Cu_2O grains was also observed by other studies [24,27]. Cu_2O branches grew vertically, resulting in a thicker Cu_2O film, thus covering the leaf-like shape of Cu_2O grains, as seen in Cu_2O deposited for 15 min (Figure 2(b)) and 25 min (Figure 2(c)). In this condition, the Cu_2O surface showed a porous structure. The leaf-like morphology of Cu_2O was no longer visible in the deposition time of 35 min (Figure 2(d)) and 45 min (Figure 2(e)). In this situation, the Cu_2O surface exhibited an irregular faceted shape with a highly dense coverage, which could be caused by the nonuniform distribution of Cu^{2+} during the electrodeposition.

Based on the analysis on the topography images, the roughness and surface area also varied with the deposition time. Under the deposition times of 5, 15, 25, 35, and 45 min, the

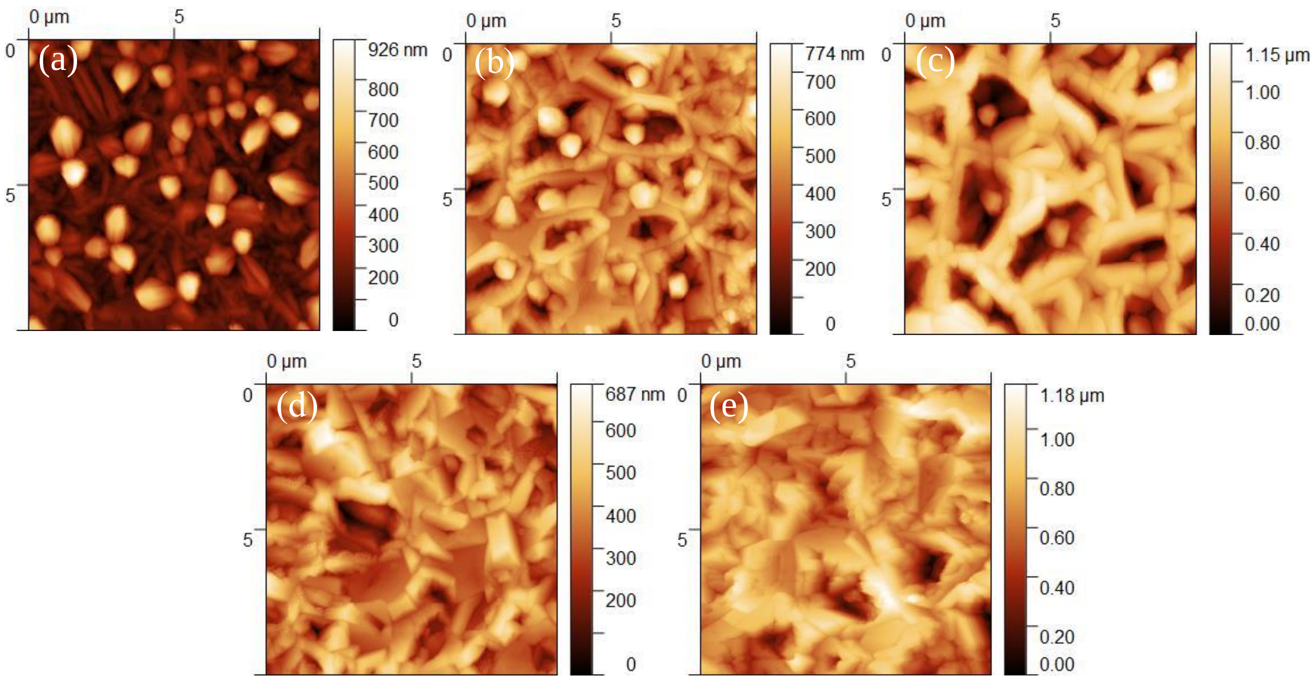

Figure 2. 2D AFM images showing topography of Cu_2O/FTO deposited under deposition times of (a) 5 min, (b) 15 min, (c) 25 min, (d) 35 min, and (e) 45 min.

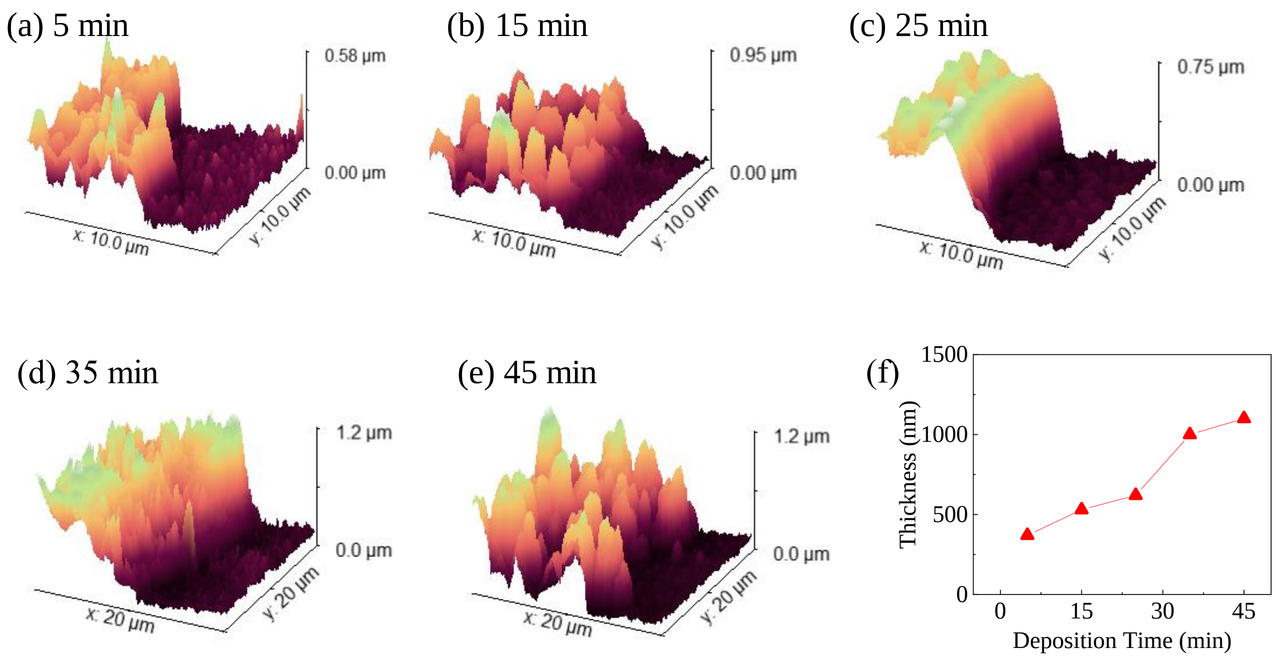

Figure 3. 3D AFM images showing thicknesses of Cu_2O on FTO substrate deposited under different deposition times.

roughnesses of Cu_2O were 151.5, 133.5, 220.7, 122.8, and 159.2 nm, respectively. Meanwhile, the surface areas were 130.3, 123.9, 133.5, 115.7, and 123.7 μm². In addition to the substrate conductivity, the variations of morphology, roughness, and surface area with the deposition time were caused by the surface diffusion of Cu^{2+} in the electrodeposition [26].

The thickness of Cu_2O on the FTO substrate was measured by AFM. However, because Cu_2O was not reflective enough, it was difficult to see the "step height" via camera (CCD) in AFM system. Hence, the Cu_2O/FTO having a "step height" was placed on top of the Au/glass so that the boundaries between FTO and Cu_2O were clearly seen because of the reflective Au/glass. Next, the position of AFM cantilever was adjusted so that it was exactly positioned on the boundary between Cu_2O and FTO. Next, AFM scanning was performed horizontally, and a "step height" profile was obtained, shown in Figure 3. In addition to better density and coverage of Cu_2O grains on the FTO surface, the thickness of the Cu_2O film increased from 370 to 1100 nm with the increasing deposition time [18,28]. This result was consistent with the increase in total charge during electrochemical deposition.

The XRD and Raman scattering were measured to identify the presence of Cu_2O on the FTO surface. Figure 4(a) shows the XRD patterns of Cu_2O/FTO deposited under different deposition times from 5 to 45 min. The XRD patterns exhibited several peaks with 2θ values of 36.58, 42.29, and 61.30°, corresponding to the (111), (200), and (220) crystal planes of pure Cu_2O (ICSD No. 98 -006-0719), respectively [3,7]. The intensity of the (111) peak was higher than those of peaks indexed to (200) and (220), indicating the preferential growth of Cu_2O along the (111) direction. The intensity of (111) and (200) peaks changed with deposition time, where increasing the deposition time increased the crystallinity in

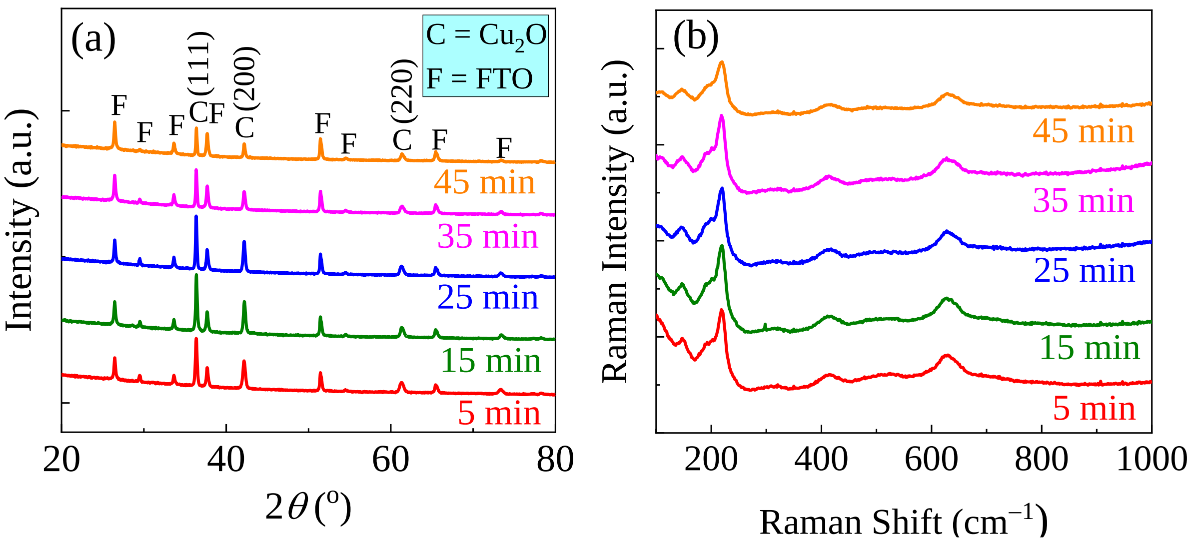

Figure 4. (a) XRD patterns and (b) Raman specta of Cu_2O/FTO deposited under different deposition times.

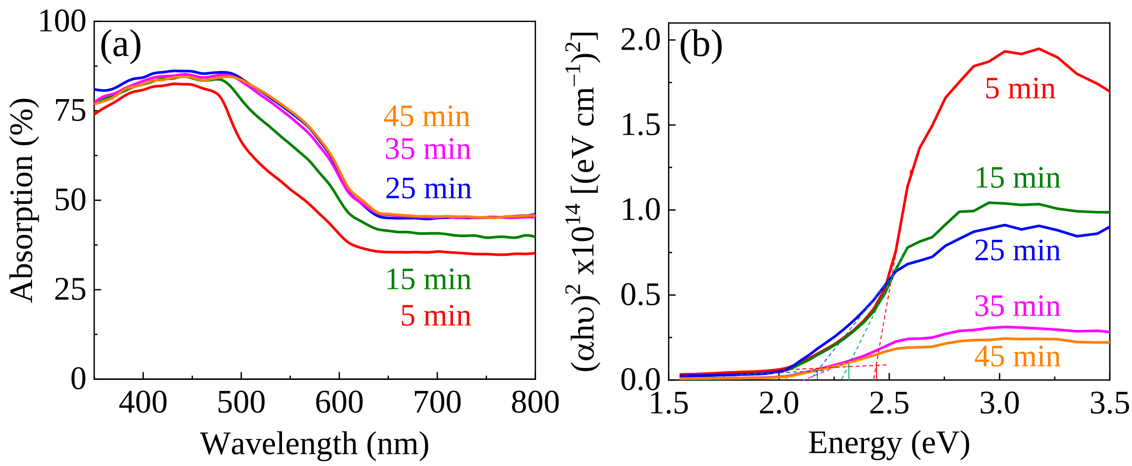

Figure 5. (a) Absorption spectra and (b) Tauc-plots of Cu_2O/FTO deposited under different deposition times.

the (111) and (200) orientations, as shown in the deposition time of Cu_2O/FTO for 5 to 25 min. However, Cu_2O/FTO deposited for 35 and 45 min showed a decrease in (111) and (200) orientations, which could attributed to the absence of leaf-like morphology in Cu_2O/FTO (see AFM images). Another peak in the XRD pattern originates from the FTO substrate. The Raman spectra of the Cu_2O/FTO are shown in Figure 4(b). Several peaks at Raman shifts of 146, 218.5, 413.7, 503.1, and 628.8 cm^{-1} were observed, corresponding to the Raman spectrum of Cu_2O [29]. The Raman peaks did not change much with the deposition times. The XRD patterns and Raman scattering spectrum confirmed that the electrodeposition of Cu_2O was successful. Only Cu_2O was grown on the FTO surface, and no other phases of copper oxide were found.

The light absorption spectra of Cu_2O/FTO were recorded using UV–vis spectroscopy. Cu_2O/FTO exhibited high light absorption in the spectral region of 350 – 600 nm, as shown in Figure 5(a), in agreement with other studies [4,24,30]. The light absorption increased as the deposition time increased. It indicated that the higher Cu_2O thickness yielded the higher light absorption, which was proportional to the amount of Cu_2O materials on the FTO substrate caused by the longer deposition time. With a higher thickness, the distribution of the intensity of the radiant energy inside the Cu_2O was also higher [20]. A red shift at the absorption edge was observed with the increasing deposition times, consistent with the Cu_2O color changing from yellow to reddish. The apparent absorption observed at wavelengths greater than 600 nm originated from light scattering losses during the measurement. Tauc-plots of Cu_2O/FTO, calculated from the absorption coefficient assuming a direct band gap, $(\alpha h\nu)^2$ [31], showed that the Cu_2O/FTO had a bandgap energy of 2.4, 2.3, 2.2, 2.1, and 2.0 eV, for deposition time of 5, 15, 25, 35, and 45 min, respectively (Figure 5(b)). With a band gap energy of around 2 eV, Cu_2O could absorb visible light from the sun [4,8]. The higher the deposition time, the longer the wavelength of light that can be absorbed.

3.2 Effect of Cu_2O Thickness on Photocatalytic Properties of Cu_2O/FTO

The current intensity of Cu_2O/FTO was measured in the electrolyte of 0.05 M Na_2SO_4 without additional bias under chopped monochromatic light irradiation of 366 and 470 nm (5 mW.cm^{-2}), shown in Figures 6(a) and 6(b). Under dark conditions, the current intensity of the

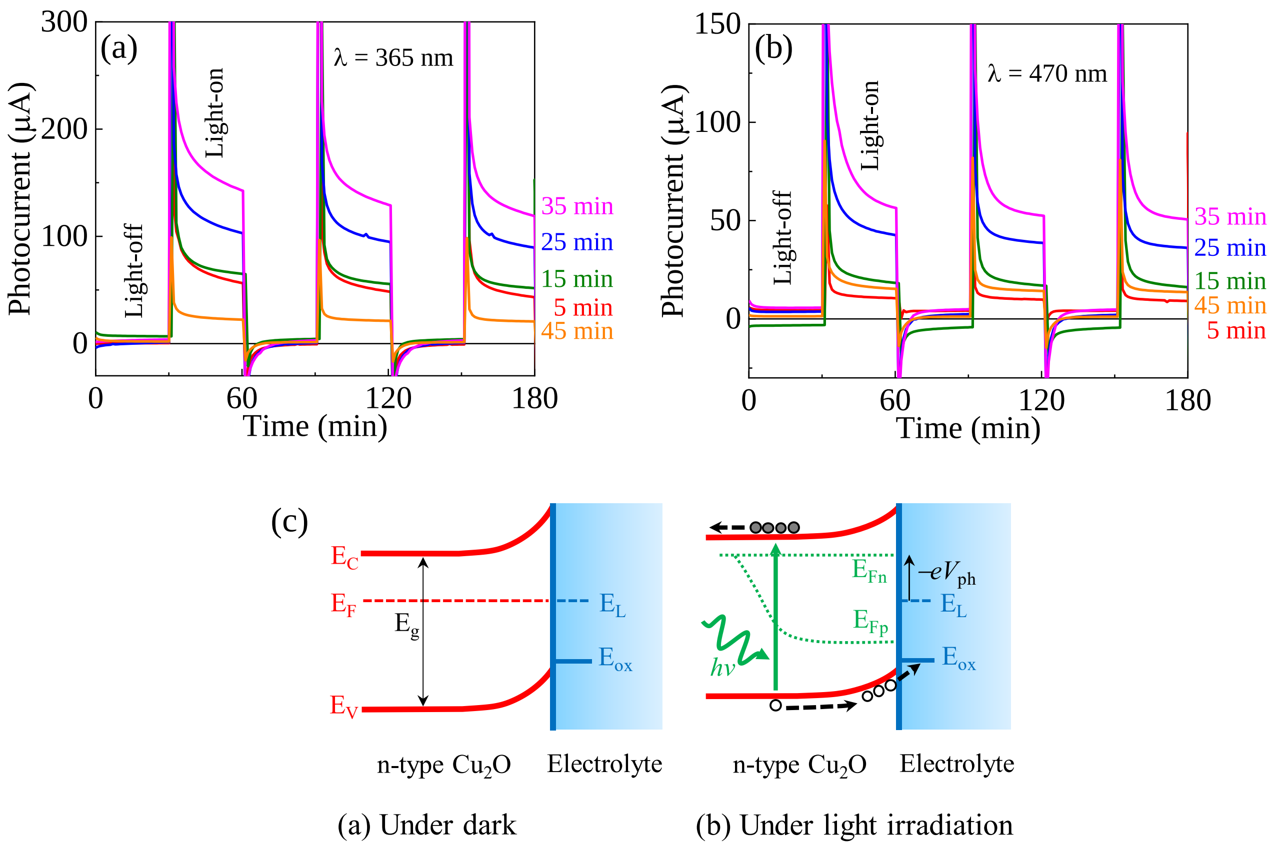

Figure 6. Photocurrent of Cu_2O/FTO deposited under different deposition times, irradiated with wavelengths: (a) 365 nm and (b) 470 nm. (c) Schematic energy band diagram of n-type Cu_2O/electrolyte under dark and light irradiation conditions [12].

Cu_2O/FTO was minuscule (<1 μA), indicating that the adsorption and catalysis were very weak and negligible without any specific analytes. Cu_2O/FTO exhibited an anodic photocurrent that increased with the increase of the deposition time but decreased after 35 min deposition time, indicating that the threshold thickness of Cu_2O was approximately 1000 nm. The anodic photocurrent is established as the behaviour of n-type semiconductors in contact with an electrolyte [11,12].

The schematic diagram of n-type Cu_2O/electrolyte under dark and irradiation conditions is illustrated in Figure 6(c) [12]. In equilibrium under dark conditions, the Fermi energy of Cu_2O (E_F) and Fermi energy of liquid water (E_L) aligned, forming a Schottky junction. Under light irradiation, the Cu_2O absorbed light with an energy higher than its band gap energy, yielding photogenerated electron-hole pairs in the Cu_2O. The photogenerated electrons were excited into the CB of Cu_2O, while the photogenerated holes remain in the VB of Cu_2O. In this situation, the E_F of Cu_2O splitted into quasi-Fermi level of electron (E_{Fn}) and quasi-Fermi level of the hole (E_{Fp}). In the photoelectrochemical cell, the photogenerated electrons in the CB moved to FTO and then transferred to the Pt plate via an external circuit. The remaining photogenerated holes in the VB were transferred to the electrolyte for the oxygen evolution reaction. Thus, an anodic photocurrent was generated [12]. The photocurrent was much higher than the dark current, indicating that the oxidation reaction in the Cu_2O/electrolyte was dominated by photocatalysis.

Determination of the correct deposition time during the Cu_2O deposition process was very important. Under irradiation of 365 nm, the photocurrent increased from 60 to 150 μA when the deposition time increased from 5 to 35 min and decreased drastically to 24 μA when the deposition time was adjusted to 45 min. The same behavior was also observed under irradiation of 470 nm. The Cu_2O/FTO deposited at 35 min exhibited the highest photocurrent (58 μA) among all the investigated Cu_2O/FTO. This means that 35 min was the suitable deposition time to prepare Cu_2O/FTO to produce the highest photocurrent. It also indicated that the suitable thickness to achieve the highest photocurrent was approximately 1000 nm. With a thickness of 1000 nm, Cu_2O had a highly dense coverage and high light absorption. The higher light absorption resulted in the higher photogenerated electron and hole, which leaded to the higher photocurrent. In addition, the charge diffusions, which were the transfers of electrons from Cu_2O to FTO and holes from Cu_2O to electrolyte, still proceed quite well [20]. The charge transfer could be characterized by electrochemical impedance spectroscopy [32]. On the other hand, the Cu_2O/FTO deposited for 45 min, having a thickness higher than 1000 nm, showed the lowest photocurrent even though the morphology of Cu_2O exhibited a highly dense coverage and the light absorption was high. It means that there was another reason causing the low photocurrent of Cu_2O/FTO deposited at 45 min. It indicated that if Cu_2O was too thick, photogenerated electrons and holes could not diffuse and transfer optimally, which mean the resistance of Cu_2O was too large. Therefore, Cu_2O/FTO with a sufficient Cu_2O thickness could produce the optimal light absorption and a good charge transfer process, resulting in highest photocurrent.

The photocatalytic activity of Cu_2O/FTO electrodeposited at 35 min was examined by

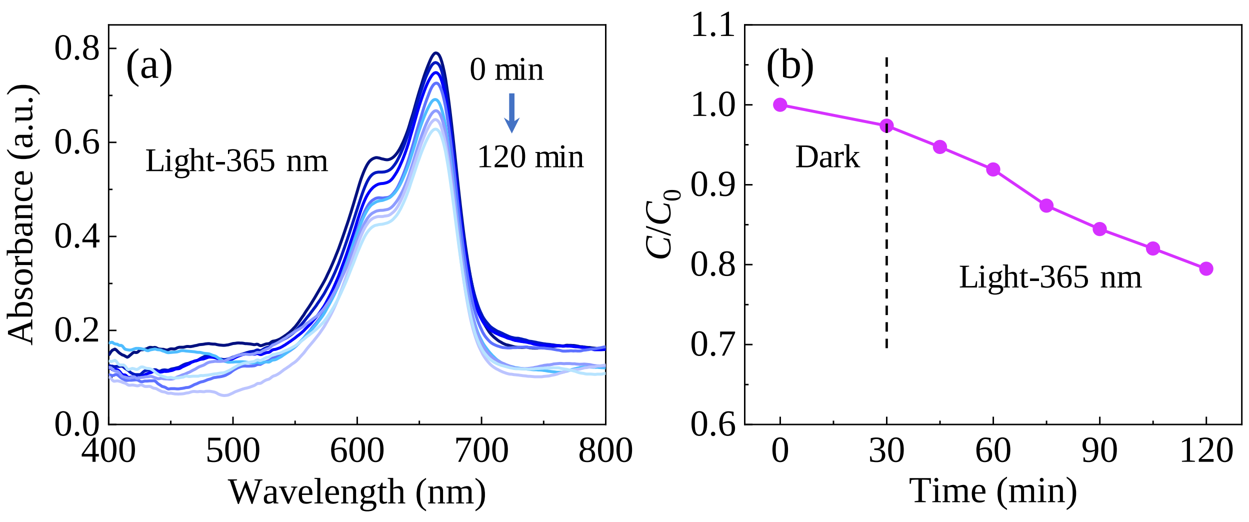

Figure 7. (a) Decrease in the MB absorbance peak by the photocatalyst of Cu_2O/FTO electrodeposited at 35 min under dark from 0 to 30 min and under light irradiation of 365 nm wavelength from 30 to 120 min. (b) Photocatalytic degradation of MB (C/C_0) by Cu_2O electrodeposited at 35 min.

measuring the degradation of MB in the electrolyte of 0.05 M Na_2SO_4 without a bias. The MB was mixed with Na_2SO_4 electrolyte to increase the conductivity of the wastewater solution containing MB. The solution conductivity could affect the current efficiency and consumption of electrical energy in the photocatalytic degradation [33]. The degradation of MB was measured by monitoring the decrease in absorbance peak of MB solution at a wavelength of 664 nm under dark for the first 30 min and light irradiation of 365 nm (38 mW cm^{-2}) for 90 min afterward (Figure 7(a)). Figure 7(b) shows the photocatalytic degradation in the MB concentration (C/C_0) by the Cu_2O/FTO. Under dark conditions, the Cu_2O/FTO could degrade the MB by approximately 2.6% in 30 min. The MB was degraded through the adsorption and catalysis processes in the dark [21]. Under light irradiation of 365 nm, the degradation percentage increased to 22.9 % for a total time of 120 min. In addition to the adsorption and catalysis processes, the MB degradation was due to the photocatalysis through photooxidation process [21,34]. Hence, the Cu_2O/FTO was a good photocatalyst for MB degradation due to the synergetic effect among the adsorption, catalysis, and photocatalysis.

The investigation on n-type Cu_2O under different deposition times provided an optimal thickness for Cu_2O photocatalyst. However, the produced photocurrent density (30 μA.cm^{-2} under irradiation of 365 nm and 11.6 μA.cm^{-2} under irradiation of 470 nm) is still low compared with the theoretical photocurrent. Theoretically, Cu_2O exhibits a solar-to-hydrogen (STH) efficiency of 18%, corresponding to the photocurrent density of 14 mA.cm^{-2} [35]. The high recombination of photogenerated charges may cause the low photocurrent of the as-prepared Cu_2O [36]. In future research, n-type Cu_2O can be combined with p-type Cu_2O to reduce the charge recombination. In addition, the photocurrent exhibited a decay with time under light irradiation (Figures 6(a) and 6(b)), indicating the poor photostability in aqueous solution [37,38]. Poor photostability is possible because Cu_2O undergoes photo-corrosion, where reduction and oxidation potentials of Cu_2O lie between the bandgap of Cu_2O [36]. Hence, annealing and protection with a capacitive coating layer can be good ways to improve the photostability of Cu_2O in future research.

4. Conclusions

The photocatalytic properties of n-type Cu_2O under different Cu_2O thicknesses were investigated. The Cu_2O was deposited on an FTO substrate using an electrochemical deposition method. The Cu_2O film thickness was controlled by adjusting the deposition time from 5 to 45 min. The quality of the Cu_2O/FTO was characterized using several techniques, consisting of AFM, XRD, Raman spectroscopy, and UV–vis spectroscopy. The Cu_2O exhibited a morphological form that depended on the deposition time, where the Cu_2O coverage become denser with the increase of deposition time. The Cu_2O thickness increased as the deposition time increased. The Cu_2O/FTO could absorb light up to a wavelength of 600 nm (band gap energy 2.0 eV). The absorption of the Cu_2O/FTO increased as the deposition time increased because of the increase in film thickness. The photocatalytic properties of the Cu_2O/FTO were investigated by measuring the photocurrent under UV and visible light irradiation. The Cu_2O/FTO demonstrated an anodic photocurrent behaviour and tended to increase with the increasing deposition time but decreased after a deposition time of 35 min, showing a threshold thickness of approximately 1000 nm. With the thickness of 1000 nm, the Cu_2O/FTO exhibited the highest anodic photocurrent, which was attributed by the optimal thickness for light absorption, highly dense of Cu_2O coverage, and quite well charge diffusion. Further increasing Cu_2O thickness, no photocurrent enhancement was obtained. The photocatalytic properties of the Cu_2O/FTO deposited at 45 min was the lowest even though the morphology showed a highly dense coverage, and the absorption was high, attributed to the relatively too-high resistance of Cu_2O that caused poor charge diffusion.

Acknowledgments

The authors would like to thank the Ministry of Science and Technology (MOST) Taiwan for their support of this research through the grants MOST 111-2112-M-029-009 and 112-2112-M-029 -005.

CRediT Author Statement

R.A.N. Khasanah: Conceptualization, Methodology, Investigation, Data Curation, Data Analysis, Writing, Review and Editing; *F.S.-S. Chien*: Conceptualization, Methodology, Supervision, Review, Resource; *R. Prasetyowati*: Review and Editing; *R. Yudianti*: Review and Supervision. All authors have read and agreed to the published version of the manuscript.

References

[1] Lin, L., Hisatomi, T., Chen, S., Takata, T., Domen, K. (2020). Visible-light-driven photocatalytic water splitting: Recent progress and challenges. *Trends in Chemistry*, 2, 813–824. DOI: 10.1016/j.trechm.2020.06.006.

[2] Nazim, M., Khan, A.A.P., Asiri, A.M., Kim, J.H. (2021). Exploring rapid photocatalytic degradation of organic pollutants with porous CuO nanosheets: Synthesis, dye removal, and kinetic studies at room temperature. *ACS Omega*, 6, 2601–2612. DOI: 10.1021/acsomega.0c04747.

[3] Khasanah, R.A.N., Lin, H.-C., Ho, H.-Y., Peng, Y.-P., Lim, T.-S., Hsiao, H.-L., Wang, C.-R., Chuang, M.-C., Chien, F.S.-S. (2021). Studies on the substrate-dependent photocatalytic properties of Cu_2O heterojunctions. *RSC Advances*, 11, 4935–4941. DOI: 10.1039/D0RA10681J.

[4] Laidoudi, S., Bioud, A.Y., Azizi, A., Schmerber, G., Bartringer, J., Barre, S., Dinia, A. (2013). Growth and characterization of electrodeposited Cu_2O thin films. *Semiconductor Science and Technology*, 28, 115005. DOI: 10.1088/0268-1242/28/11/115005.

[5] Khasanah, R.A.N., Lin, H.-C., Ho, H.-Y., Peng, Y.-P., Hsiao, H.-L., Wang, C.-R., Chien, F.S.-S. (2022). Photoelectrocatalytic hydrolysis of ammonia borane by electrochemical deposited cuprous oxide on titanium dioxide nanotube arrays. *International Journal of Hydrogen Energy*, 47, 11203–11210. DOI: 10.1016/j.ijhydene.2022.01.167.

[6] Koiki, B.A., Arotiba, O.A. (2020). Cu_2O as an emerging semiconductor in photocatalytic and photoelectrocatalytic treatment of water contaminated with organic substances: A review. *RSC Advances*, 10, 36514–36525. DOI: 10.1039/D0RA06858F.

[7] Hossain, M.A., Al-Gaashani, R., Hamoudi, H., Al Marri, M.J., Hussein, I.A., Belaidi, A., Merzougui, B.A., Alharbi, F.H., Tabet, N. (2017). Controlled growth of Cu_2O thin films by electrodeposition approach. *Materials Science in Semiconductor Processing*, 63, 203–211. DOI: 10.1016/j.mssp.2017.02.012.

[8] Bagal, I.V., Chodankar, N.R., Hassan, M.A., Waseem, A., Johar, M.A., Kim, D.-H., Ryu, S.-W. (2019). Cu_2O as an emerging photocathode for solar water splitting - a status review. *International Journal of Hydrogen Energy*, 44, 21351–21378. DOI: 10.1016/j.ijhydene.2019.06.184.

[9] Son, M.-K. (2021). Design and demonstration of large scale Cu_2O photocathodes with metal grid structure for photoelectrochemical water splitting. *Energies*, 14, 7422. DOI: 10.3390/en14217422.

[10] McShane, C.M., Choi, K.-S. (2009). Photocurrent enhancement of n-type Cu_2O electrodes achieved by controlling dendritic branching growth. *Journal of the American Chemical Society*, 131, 2561–2569. DOI: 10.1021/ja806370s.

[11] Chen, Y.-C., Chen, Y.-J., Dong, P.-H., Hsu, Y.-K. (2020). Benchmarked photoelectrochemical water splitting by nickel-doped n-type cuprous oxide. *ACS Applied Energy Materials*, 3, 1373–1380. DOI: 10.1021/acsaem.9b01781.

[12] Khasanah, R.A.N., Lee, C.-H., Li, Y.C., Chen, C.-H., Lim, T.-S., Wang, C.-R., Chang, P.-Y., Sheu, H.-S., Chien, F.S.-S. (2022). Enhancement of photocatalytic activity of electrodeposited Cu_2O by reducing oxygen vacancy density. *ACS Applied Energy Materials*, 5, 15326–15332. DOI: 10.1021/acsaem.2c02963.

[13] Dolai, S., Das, S., Hussain, S., Bhar, R., Pal, A.K. (2017). Cuprous oxide (Cu_2O) thin films prepared by reactive d.c. Sputtering technique. *Vacuum*, 141, 296–306. DOI: 10.1016/j.vacuum.2017.04.033.

[14] Karapetyan, A., Reymers, A., Giorgio, S., Fauquet, C., Sajti, L., Nitsche, S., Nersesyan, M., Gevorgyan, V., Marine, W. (2015). Cuprous oxide thin films prepared by thermal oxidation of copper layer. Morphological and optical properties. *Journal of Luminescence*, 159, 325–332. DOI: 10.1016/j.jlumin.2014.10.058.

[15] Saadaldin, N., Alsloum, M.N., Hussain, N. (2015). Preparing of copper oxides thin films by chemical bath deposition (CBD) for using in environmental application. *Energy Procedia*, 74, 1459–1465. DOI: 10.1016/j.egypro.2015.07.794.

[16] Abdelfatah, M., Ledig, J., El-Shaer, A., Sharafeev, A., Lemmens, P., Mosaad, M.M., Waag, A., Bakin, A. (2016). Effect of potentiostatic and galvanostatic electrodeposition modes on the basic parameters of solar cells based on Cu_2O thin films. *ECS Journal of Solid State Science and Technology*, 5, Q183–Q187. DOI: 10.1149/2.0191606jss.

[17] Rahal, H., Kihal, R., Affoune, A.M., Rahal, S. (2020). Effect of solution pH on properties of cuprous oxide thin films prepared by electrodeposition from a new bath. *Journal of Electronic Materials*, 49, 4385–4391. DOI: 10.1007/s11664-020-08093-y.

[18] Mohd Hanif, A.S., Azmal, S.A., bin Ahmad, M.K., Mohamad, F. (2015). Effect of deposition time on the electrodeposited n-Cu_2O thin film. *Applied Mechanics and Materials*, 773, 677–681. DOI: 10.4028/www.scientific.net/AMM.773-774.677.

[19] Kalubowila, K.D.R.N., Gunawardhana, L.K.A.D.D.S., Wijesundera, R.P., Siripala, W. (2014). Methods for improving n-type photoconductivity of electrodeposited Cu_2O thin films. *Semiconductor Science and Technology*, 29, 075012. DOI: 10.1088/0268-1242/29/7/075012.

[20] Camera-Roda, G., Santarelli, F. (2007). Optimization of the thickness of a photocatalytic film on the basis of the effectiveness factor. *Catalysis Today*, 129, 161–168. DOI: 10.1016/j.cattod.2007.06.062.

[21] Osorio-Aguilar, D.-M. (2023). Saldarriaga-Noreña, H.-A., Murillo-Tovar, M.-A., Vergara-Sánchez, J., Ramírez-Aparicio, J., Magallón-Cacho, L., García-Betancourt, M.-L. Adsorption and photocatalytic degradation of methylene blue in carbon nanotubes: A review with bibliometric analysis. *Catalysts*, 13, 1480. DOI: 10.3390/catal13121480.

[22] Qi, G., Liu, M., Tang, C., Chang, J., Yang, C., Liu, F., Ning, X., Yang, Y. (2021). Conductivity controlling of Cu_2O film photoelectrode for water splitting by a novel electrochemical approach - differential potentiostatic deposition. *International Journal of Hydrogen Energy*, 46, 2878–2889. DOI: 10.1016/j.ijhydene.2020.04.176.

[23] Ait Hssi, A., Atourki, L., Labchir, N., Ouafi, M., Abouabassi, K., Elfanaoui, A., Ihlal, A., Bouabid, K. (2020). Optical and dielectric properties of electrochemically deposited p-Cu_2O films. *Materials Research Express*, 7, 016424. DOI: 10.1088/2053-1591/ab6772.

[24] Yang, Y., Han, J., Ning, X., Cao, W., Xu, W., Guo, L. (2014). Controllable morphology and conductivity of electrodeposited Cu_2O thin film: Effect of surfactants. *ACS Applied Materials & Interfaces*, 6, 22534–22543. DOI: 10.1021/am506657v.

[25] Yu, X., Tang, X., Li, J., Zhang, J., Kou, S., Zhao, J., Yao, B. (2017). Nucleation mechanism and optoelectronic properties of Cu_2O onto ito electrode in the electrochemical deposition process. *Journal of The Electrochemical Society*, 164, D999–D1005. DOI: 10.1149/2.1081714jes.

[26] Brandt, I.S., Zoldan, V.C., Stenger, V., Plá Cid, C.C., Pasa, A.A., Oliveira, T.J., Aarão Reis, F.D.A. (2015). Substrate effects and diffusion dominated roughening in Cu_2O electrodeposition. *Journal of Applied Physics*, 118, 145303. DOI: 10.1063/1.4932642.

[27] Wang, P., Wu, H., Tang, Y., Amal, R., Ng, Y.H. (2015). Electrodeposited Cu_2O as photoelectrodes with controllable conductivity type for solar energy conversion. *Journal of Physical Chemistry C*, 119, 26275–26282. DOI: 10.1021/acs.jpcc.5b07276.

[28] Taher, S.J., Barzinjy, A.A., Hamad, S.M. (2020). The effect of deposition time on the properties of Cu_2O nanocubes using an electrochemical deposition method. *Journal of Electronic Materials*, 49, 7532–7540. DOI: 10.1007/s11664-020-08495-y.

[29] Benz, J., Hering, K.P., Kramm, B., Polity, A., Klar, P.J., Siah, S.C., Buonassisi, T. (2017). The influence of nitrogen doping on the electrical and vibrational properties of Cu_2O. *Physica Status Solidi B*, 254, 1600421. DOI: 10.1002/pssb.201600421.

[30] Chen, A., Long, H., Li, X., Li, Y., Yang, G., Lu, P. (2009). Controlled growth and characteristics of single-phase Cu_2O and CuO films by pulsed laser deposition. *Vacuum*, 83, 927–930. DOI: 10.1016/j.vacuum.2008.10.003.

[31] Elmahdy, M.M., El-Shaer, A. (2019). Structural, optical and dielectric investigations of electrodeposited p-type Cu_2O. *Journal of Materials Science: Materials in Electronics*, 30, 19894-19905. DOI: 10.1007/s10854-019-02356-z.

[32] Lopes, T., Andrade, L., Le Formal, F., Gratzel, M., Sivula, K., Mendes, A. (2014). Hematite photoelectrodes for water splitting: Evaluation of the role of film thickness by impedance spectroscopy. *Physical Chemistry Chemical Physics*, 16, 16515–16523. DOI: 10.1039/C3CP55473B.

[33] Lemlikchi, W., Khaldi, S., Mecherri, M.O., Lounici, H., Drouiche, N. (2012). Degradation of disperse red 167 AZO dye by bipolar electrocoagulation. *Separation Science and Technology*, 47, 1682–1688. DOI: 10.1080/01496395.2011.647374

[34] Anantha, M.S., Olivera, S., Hu, C., Jayanna, B.K., Reddy, N., Venkatesh, K., Muralidhara, H.B., Naidu, R. (2020). Comparison of the photocatalytic, adsorption and electrochemical methods for the removal of cationic dyes from aqueous solutions. *Environmental Technology & Innovation*, 17, 100612. DOI: 10.1016/j.eti.2020.100612.

[35] Jiang, C., Moniz, S.J.A., Wang, A., Zhang, T., Tang, J. (2017). Photoelectrochemical devices for solar water splitting – materials and challenges. *Chemical Society Reviews*, 46, 4645–4660. DOI: 10.1039/C6CS00306K.

[36] Toe, C.Y., Scott, J., Amal, R., Ng, Y.H. (2019). Recent advances in suppressing the photocorrosion of cuprous oxide for photocatalytic and photoelectrochemical energy conversion. *Journal of Photochemistry and Photobiology C: Photochemistry Reviews*, 40, 191–211. DOI: 10.1016/j.jphotochemrev.2018.10.001.

[37] Nandjou, F., Haussener, S. (2022). Modeling the photostability of solar water-splitting devices and stabilization strategies. *ACS Applied Materials & Interfaces*, 14, 43095–43108. DOI: 10.1021/acsami.2c08204.

[38] Yang, Y., Han, J., Ning, X., Su, J., Shi, J., Cao, W., Xu, W. (2016). Photoelectrochemical stability improvement of cuprous oxide (Cu_2O) thin films in aqueous solution. *International Journal of Energy Research*, 40, 112–123. DOI: 10.1002/er.3328.